Spatial statistical smoothing function to analytical data from cerebral blood flow imaging

Tomoaki Yamamoto[1] MHSc,
Etsuo Miyaoka[2] PhD,
Toshi Hashimoto[3] MD,
Masahisa Onoguchi[4] PhD

1. *Department of Radiological Sciences, International University of Health and Welfare, Tochigi, Japan*
2. *Department of Mathematics, Tokyo University of Science, Tokyo, Japan*
3. *Department of Radiology, Showa University Fujigaoka Hospital, Kanagawa, Japan*
4. *Kanazawa University Graduate School of Medical Science, Kanazawa, Japan*

Keywords: Spatial statistics – Smoothing function – SPET – Z score – Cerebral blood flow

Correspondence address:
Tomoaki Yamamoto MHSc,
Department of Radiological Sciences,
International University of Health and Welfare 2600-1,
Kitakanemaru Otawara-city,
Tochigi, 324-8501, Japan
Tel: +81287243127,
E-mail: tyamamoto@iuhw.ac.jp

Received:
05 October 2009
Accepted revised:
26 October 2009

Abstract

Spatial statistics is widely used in fields where analysis of large-scale distributions is performed, such as synoptic meteorology and geostatistics. We constructed a smoothing function as part of a fundamental study aimed at introducing spatial statistics to the Z score map of cerebral blood flow-single photon emission tomography (CBF-SPET) and examined the applicability of spatial statistics to CBF-SPET imaging. The free statistical processing language R was chosen as the development language, and the smoothing function was constructed by use of a kernel function, a thin-plate spline function, and the Bayesian method. A Gaussian function was used as the kernel function, and three values for the smoothing parameters (0.25, 0.5, standard deviation (SD)) were used. Furthermore, the smoothing parameters of the thin-plate spline function were estimated by use of generalized cross validation (GCV), the Gibbs sampling method was adopted for the Bayesian method, and the number of iterations and the value for the burn-in were set to 500 and 250, respectively. In performing the visual assessment of the source image and the smoothed image, there were no differences caused by the smoothing process. However, there were discrepancies in the contour map at each step of the smoothing iteration. Comparing the residual sum of squares of the source image and the resulting image after each smoothing iteration, the minimum and maximum values for the image after processing with a kernel function were 1.329×10^{-11} and 21.96 when the smoothing parameters were 0.25 and SD, respectively. The smoothing function, which was examined for the purpose of applying the spatial statistical method to CBF-SPET imaging, successfully performed a smoothing without generating visible discrepancies when compared with the source image. *In conclusion*, our research showed that spatial statistics as performed by us is applicable as an analytical method for better cerebral blood flow-SPET imaging.

Hell J Nucl Med 2009; 12(3) : 229-233 • Published on line: 14 November 2009

Introduction

Image analysis techniques in the diagnosis of dementia are advancing rapidly, and magnetic resonance imaging (MRI) and cerebral blood flow-single photon emission tomography (CBF-SPET), as well as ^{18}Fluorine-fluorodeoxyglucose positron emission tomography (^{18}F-FDG-PET), are important instruments for early diagnosis of dementia. Regarding diagnostic techniques based on imaging, which are used for extracting information from the obtained images, it is necessary to construct analytical methods, which can be used for attaining higher sensitivity and specificity and for improving the predictability of the development of clinical conditions.

In the CBF-SPET imaging analysis method for Alzheimer's disease (AD), it is possible to verify in the early disease stages whether there is decreased blood flow in the posterior cingulate gyrus precuneus by using a normalcy database for comparison. These methods have been clarified through objective evaluation of the Z score by performance of statistical processing of the normalcy database and of clinical cases [1-5]. Three methods (statistical parametric mapping; SPM, three-dimensional stereotactic surface projection; 3D-SSP, and easy Z score imaging system; eZIS) are conventionally accepted as representative [6-13]. The relevant literature also states that the quantitative evaluation of CBF-SPET is important in diagnosing dementia. Therefore, in the present study, we focused on the Z score map for CBF-SPET. We applied spatial statistics as used in synoptic meteorology and geostatistics to the Z score map, which can be expressed as a typical aberration area in the CBF as seen with CBF-SPET, after which we examined the smoothing function necessary for performing spatial statistic analysis of the distribution in the aberrant area and explored its applicability to CBF-SPET imaging.

Equipment and methods

Preparation of the imaging data

The clinical data were chosen at random from outpatients who were examined at a neurological clinic, and among the patients who received a CBF-SPET examination, the consent of a 67 years old female patient with her family was obtained with regard to using the technetium-99m ethyl cysteinate dimmer (^{99m}Tc-ECD; Fujifulm RI Pharma Co., LTD., Tokyo, Japan) CBF-SPET images for research purposes. The equipment used was Prism3000XP (Shimadzu Medical Systems Corporation, Kyoto, Japan) and a low-energy high-resolution fan beam collimator. The patient was lying face up with eyes closed inside the test device, and 600MBq ^{99m}Tc-ECD were administered intravenously. The patient was allowed to open her eyes after 10min of lying still, and the examination was performed 20min after the administration of ^{99m}Tc-ECD. The examination room was dim, and the silence was kept under the examination. The conditions regarding the collection of data are shown in Table 1. Using iSSP (Nihon Medi-Physics Co., LTD., Tokyo, Japan), which is an interface program to 3D-SSP, together with the obtained CBF-SPET image, we acquired the Z score map as compared with the normalcy database. The Z score of the plane of the right brain surface was outputted as text data. The depth coordinate of the data was reduced by 1, and the Z score map as converted to two dimensions was used as the source image. This source image was smoothed in accordance with the theory described below, and the result was taken as the smoothed image.

Table 1. *CBF-SPET examination protocol*

Matrix size	128x128 (3.67mm/pixel)
Acquisition mode	continuous
Acquisition angle	120 deg.x3 (3deg/step)
Acquisition time	20min (30sec/step)
Attenuation correction	Chang's method (0.13cm^{-1})
Scatter correction	none
Radiopharmacy	^{99m}Tc-ECD
Injection dose	600MBq/3ml

^{99m}Tc-ECD: technetium-99m ethyl cysteinate dimmer

Theory behind the smoothing process

Among the smoothing functions widely used in spatial statistics, three functions, which were regarded as suitable for the purposes of the research were utilized for constructing three different theories. The theories are presented below [14-21].

Kernel function

For the purpose of determining the degree of similarity between the source and the smoothed images, the Gaussian function is most widely used as a kernel function. Considering a point X and its neighboring points X_i, the Gaussian kernel K is expressed as follows:

$$K(X - X_i) = exp\left[-\frac{\|X - X_i\|}{\lambda}\right]. \quad (1)$$

Here, λ is the smoothing parameter, and it determines the size of the neighboring region. If the concentration of each point is taken as the Z score map, and if the smoothing is performed with a kernel function, it is possible to estimate the Nadaraya-Watson weight of each point by use of $\hat{f}_\lambda(X)$. In this case, d_{ij} is the Z score (the concentration) of each point, where i and j represent the pixel numbers in the direction of the x and y axes, respectively. And m and n represent the pixel size of each image.

$$\hat{f}_1(X) = \frac{\sum_{i=1}^{m}\sum_{j=1}^{n} k\left(\frac{X - X_{ij}}{\lambda}\right) d_{ij}}{\sum_{i=1}^{m}\sum_{j=1}^{n} k\left(\frac{X - X_{ij}}{\lambda}\right)}. \quad (2)$$

Apart from the choice of the kernel function, the setting of the smoothing parameter also exerts an influence on the image. In this research, the smoothing parameter was taken as 0.25, 0.5, or the standard deviation (SD) of the source image.

Thin-plate spline function

The thin-plate spline function was designed by Duchon [22]. The observed concentration y_{ij} is assumed to be the sum of the estimated value f_{ij} and the error ε_{ij}. Therefore, the concentration for each point is estimated through appropriate cross-validation such that the thin-plane spline function $S(y_{ij})$ becomes smallest.

$$y_{ij} = f_{ij} + \varepsilon_{ij} \quad i = 1, 2, \Lambda, m \quad j = 1, 2, \Lambda, n \quad (3)$$

$$S(y_{ij}) = \sum_{i=1}^{m}\sum_{j=1}^{n}(y_{ij} - f_{ij})^2 + \lambda\iint\left[\left(\frac{\partial^2 f}{\partial x^2}\right)^2 + 2\left(\frac{\partial^2 f}{\partial x \partial y}\right) + \left(\frac{\partial^2 f}{\partial y^2}\right)^2\right] dxdy. \quad (4)$$

In the case of cross-validation, a thin-plate spline function $S^{(k,l)}(y_{ij})$ is considered where the k and l values are removed:

$$S^{(k,l)}(y_{ij}) = \sum_{\substack{i=1 \\ i\neq k}}^{m}\sum_{\substack{j=1 \\ j\neq l}}^{n}(d_{ij} - f_{ij})^2 + \lambda\iint\left[\left(\frac{\partial^2 f}{\partial x^2}\right)^2 + 2\left(\frac{\partial^2 f}{\partial x \partial y}\right) + \left(\frac{\partial^2 f}{\partial y^2}\right)^2\right] dxdy. \quad (5)$$

We calculate the minimum value $f(f_\lambda^{(k,l)})$ of this $S^{(k,l)}(y_{ij})$. In this case, λ is taken as the minimum value of the ordinary cross-validation function $V_0(\lambda)$:

$$V_0(\lambda) = \frac{1}{mn}\sum_{\substack{i=1 \\ i\neq k}}^{m}\sum_{\substack{j=1 \\ j\neq l}}^{n}(d_{ij} - f_{ij})^2 \quad (6)$$

Here, we considered the generalized cross-validation function $T(\lambda)$, which is a generalized version of the ordinary cross-validation function, and λ is the estimated squared error:

$$T(\lambda) = \frac{1}{mn}\sum_{\substack{i=1 \\ i\neq k}}^{m}\sum_{\substack{j=1 \\ j\neq l}}^{n}\left(f_\lambda^{(i,j)} - f_{ij}\right)^2 \quad (7)$$

λ can be calculated as the value, which minimizes $T(\lambda)$. In the present research, λ is 9.1×10^{-6}.

Bayesian method

It is assumed that the concentration d_{ij} of each point is a sum

of the error ε_{ij} and the concentration y_{ij}.

$$y_{ij} = d_{ij} + \varepsilon_{ij} \quad i = 1, 2, \Lambda, m \quad j = 1, 2, \Lambda, n \tag{8}$$

According to the theory presented by Bayes, the posterior probability is written as follows. Where, y is the concentration of the source image, θ is the model parameter, and $f(\theta)$ is the posterior probability:

$$f(\theta|y) = \frac{f(y|\theta)\, f(\theta)}{\int f(y|\theta)\, f(\theta)\, d\theta}. \tag{9}$$

From this, by use of the estimated maximum posterior probability, the model parameter θ for which the posterior probability is maximized can be estimated through the relation $f(\theta|y) \propto f(y|\theta) f(\theta)$. Furthermore, there are necessary assumptions regarding the posterior probability, and the present data were considered to follow a normal distribution in accordance with the following equation:

$$f(y_{ij}|d_{ij}) = \frac{1}{\sqrt{2\pi\sigma^2}} exp\left[-\frac{(y_{ij}-d_{ij})^2}{2\sigma^2}\right], \quad \varepsilon_{ij} \sim N(0, \sigma^2) \tag{10}$$

$$f(d_{ij}) = \frac{1}{\sqrt{2\pi\sigma_{ij}^2}} exp\left[-\frac{(d_{ij} - \mu_{ij})^2}{2\sigma_{ij}^2}\right] \tag{11}$$

Where, μ_{ij} and σ_{ij}^2 are the mean value and the distribution of d_{ij}, respectively. Furthermore, although it is generally possible to express the noninformative prior distribution by using the Gamma function with the parameter set to a low value, in this case the parameter was set to 0.0001, as shown in the following formula:

$$\begin{aligned} \frac{1}{\sigma_{ij}^2} &= Gamma(0.0001, 0.0001) \\ \frac{1}{\sigma^2} &= Gamma(0.0001, 0.0001) \end{aligned} \tag{12}$$

However, because it is impossible to calculate the denominator in Eq. (9) analytically, we applied the Gibbs sampling method to the computation, which follows a Markov-chain Monte Carlo method. The algorithm of the Gibbs sampling method involves the selection of an initial value θ^0, after which a sampling process is iterated a finite number of times by taking θ^0 as the starting point, and a sample θ is constructed. One sample is extracted at the t+1 stage after t recursive computations are performed, this process is repeated the same number of times as the number of variables, and the t+1st sample group is obtained. The joint probability is obtained from the above, and it is applied to the denominator in Eq. (9).

Data processing

The SPET data were prepared as transverse images in a routine examination. The images were transferred to a PC, after which a Z score map was prepared with iSSP. The database at Chiba University, which was prepared with the same equipment as that used in the present research, was used as the normalcy database necessary for preparing the Z score map.

For the purpose of simplifying the computation, we selected the plane of the right brain surface among the 8 directions in which the Z score map is prepared, which was subsequently converted into text data. From the *x*, *y* and *z* axes, the axis corresponding to the depth direction was removed, and the smoothing was performed with respect to the plane formed by the *x* and *y* axes. The programming for these operations was implemented by use of the free statistical programming language R. The text data corresponding to the source image and the smoothed image were converted back to graphics, after which the changes in the area of the Z score were evaluated visually by use of a contour map. Furthermore, as an objective evaluation, the residual sum of squares (RSS) for the source image was calculated.

Results

The source image and the smoothed image represented as two-dimensional data converted back to graphics are shown in Figure 1. The value of SD in this case was 0.84. Although subtle differences appear along the periphery of the smoothed image, it is clear that there are virtually no visual differences between the smoothed image and the source one. Figure 2 presents the contour maps of the images in Figure 1. Following the increase in the value of the parameter, the contour lines became denser in the image smoothed with the kernel function (Figs. 2a, 2b and 2c), and the densest distribution was obtained for the image smoothed with the thin-plane spline function shown in (Fig. 2d). Although the contour lines for the brain surface of source image shown in (Fig. 2f) was similar to the image shown in (Fig. 2e) for the Bayesian method, the distribution corresponding to the space outside the brain surface (background) was considered to be affected by noise. The images resulting from the fusion of the images in Figures 1 and 2 are shown in Figure 3. In all cases, the shaded areas in the images mostly coincided with the contour lines upon visual examination. However, as a common feature

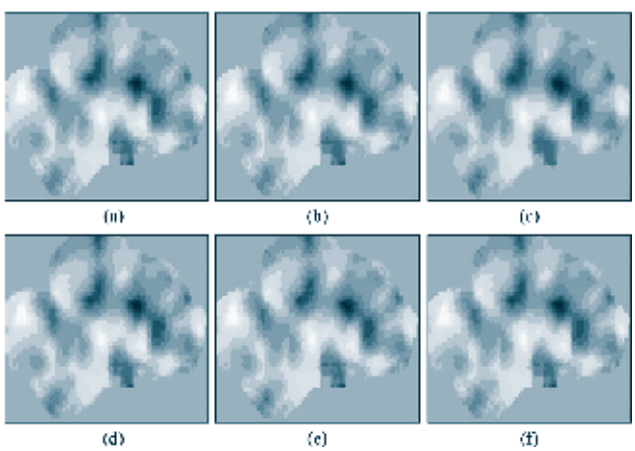

Figure 1. CBF-SPET Z score maps of the source image and the smoothed images. (a)-(c) correspond to the image smoothed with the kernel function, where the parameter values are 0.25, 0.5, and the standard deviation (SD), respectively. (d) corresponds to the thin-plane spline function, (e) corresponds to the Bayesian method, and (f) is the source image.

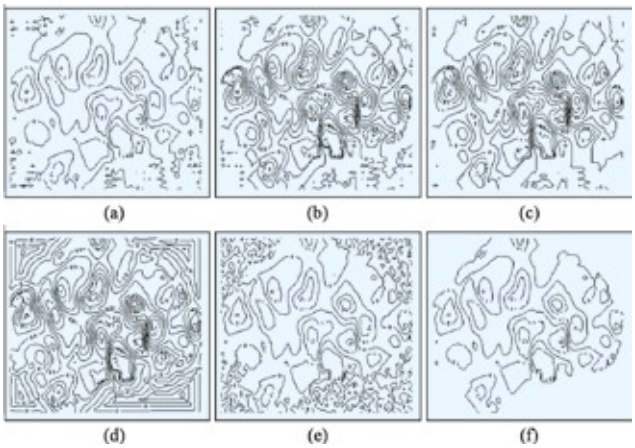

Figure 2. Contour maps of the source image and the smoothed images. The arrangement of (a)-(f) is the same as that in Figure 1.

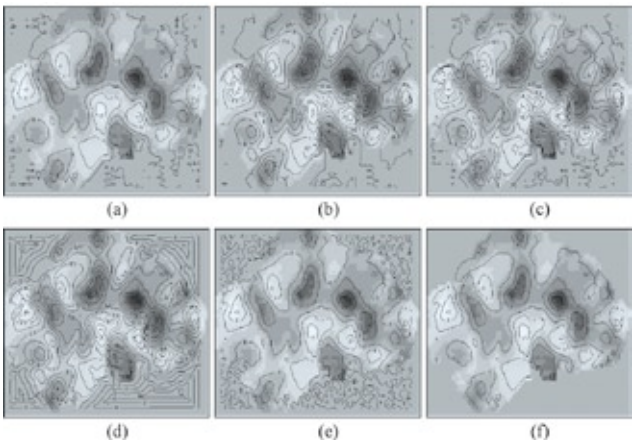

Figure 3. Images resulting from the fusion of the CBF-SPET Z score maps with the contour maps. The arrangement of (a)-(f) is the same as that in Figures 1 and 2.

shared by all images, the background was smoothed as space, which was continuous with the brain surface. The parameters of the smoothed images corresponding to the source image, as well as the computational results for the residual sum of squares, are shown in Table 2.

Table 2. *Parameters and the residual sum of squares of the smoothed images corresponding to the source image*

Smoothing function	Smoothing parameter	Residual sum square
Kernel function (0.25)	0.25	1.329×10^{-11}
Kernel function (0.50)	0.50	0.3182
Kernel function (SD)	0.84	21.96
Thin plate spline function	9.1×10^{-6}	5.843
Bayesian method	–	2.677

SD: standard deviation

Discussion

Spatial statistics, applied to synoptic meteorology analysis, is considered applicable to lesion distribution pattern analysis or quantitative analysis of the region by replacing the surface of the brain with a spherical surface. iSSP, a CBF-SPET analysis method, is considered easily applicable to spatial statistics since it projects a Z score onto the brain surface, and is consequently used as the source data this time. The smoothing function essential for a spatial statistics approach is necessary for obtaining a correlation of points in the vicinity of the brain surface and also has the strongest effects on the results. The absolute conditions fixing the smoothing function are that the data handled by the smoothing function must not show a visual change. The concern with visual changes is that diagnosis could be adversely affected. Here, 3 smoothing functions were chosen as being suitable for this study for the following reason. Using a Gaussian kernel function is a basic statistical concept and a fundamental method. The thin-plate spline function applies a conversion from 3-D to 2-D, making linear calculations possible by determining these parameters, and a detailed, smoother distribution of results can be expected [23]. As such, the Bayesian method parameters are theoretically calculable from the estimated maximum posterior probability and these are the most popular methods, which apply several natural phenomena [14].

The smoothing function used this time had no visual influence in any of the cases. However, since the compactness of the contour lines varied due to smoothing function, the degree of correlation of near points differed. Even though the kernel function method is simple, the density of contour lines varies due to the unreliable method for determining parameters, and is consequently considered difficult to put forward as a theoretical method. The density of contour lines in the thin-plate spline function becomes too high, which could make analyzing the lesion distribution from poor quality nuclear medicine images complex, and thus a more detailed examination of assessment methods is necessary after being handled by a smoothing function. Observational assessment of the lesion region in the Bayesian method do not differ much, so parameter fixing through the estimated maximum posterior probability is theoretically possible and is considered most applicable to nuclear medicine examinations such as CBF-SPET. A report by Besagg gives an example of an analysis using the Bayesian method with a planar Gamma-ray camera image, which provides a lesion profile curve from the differences in parameters [24]. Expanding the profile curve in 2-D is considered sufficient to apply it to the SPET region in spatial statistics.

There were limitations to this investigation. One was that the boundary between the brain surface and background was not distinguishable since the background was not excluded from the calculation. From the outset, the smoothing function tends to blur the margins. Therefore, it is necessary to examine a method of handling the boundary limit separately. Another limitation, which also depends on computer capabilities, is that as the calculation time for the Bayesian method took about an hour, consequently a consideration of high speed operations is necessary, as are further investiga-

tions into its practical use. In addition, each RSS value is excluded when SD is performed on the kernel function parameters to give a sufficiently low value; however, if it were excluded from the background handling calculation, it could yield a more accurate assessment. Based on the above, approaching CBF-SPET from a spatial statistical analysis, the Bayesian method is likely to be optimal for the necessary smoothing function.

From the cases chosen as the target of this research, there was only one example of a case with areas of significant reduction in blood flow, which was in the lower region of the right temporal lobe. Thus, many similar cases need to be accumulated in order to compare pathogenesis. If the mean values and dispersion of the Z score distribution in similar pathogenic cases are obtained, probabilistic diagnostic results are likely to be possible from the pathogenesis distribution. Hereafter, we plan to address the limitations of this research and to conduct clinical evaluations.

CBF-SPET is a useful technique for the early detection of dementia. In addition to increasing the accuracy of the examination or the prognosis of the disease stage, it is necessary to construct image-analysis techniques with higher degrees of objectivity. Although the calculation of Z score maps is a method of superior objectivity, it involves voxel-by-voxel analysis and does not consider the area of the disease. In order to show the areas specific to dementia and change them in accordance with the stage of the disease, one should evaluate the changes in the area in a time-series manner. Such an evaluation method coincides with the way of thinking of spatial statistics. It was found that the smoothing functions considered in this research are capable of processing the source image in such a way that there are no visible changes in Z score maps, and it is possible to take an approach based on spatial statistics.

In conclusion, we found that the smoothing functions considered in this research are capable to increasing the accuracy of the CBF-SPET examination for the early detection of dementia or for the prognosis of the disease stage.

Bibliography

1. Imon Y, Matsuda H, Ogawa M, Kogure O, Sunohara N. SPECT image analysis using statistical parametric mapping in patients with Parkinson's disease. *J Nucl Med* 1996; 40: 1583-1589.
2. Minoshima S, Giordani B, Berent S et al. Metabolic reduction in the posterior cingulated cortex in very early Alzheimer's disease. *Ann Neurol* 1997; 42: 85-94.
3. Tanaka M, Fukuyama H, Yamauchi H et al. Regional cerebral blood flow abnormalities in nondemented patients with memory impairment. *J Neuroimaging* 2000; 12: 112-118.
4. Hanyu H, Shimizu T, Tanaka Y et al. Effect of age on regional cerebral blood flow patterns in Alzheimer's disease patients. *J Neuro Sci* 2002; 209: 25-30.
5. Hirao, K, Ohnishi T, Hirata Y et al. The prediction of rapid conversion to Alzheimer's disease in mild cognitive impairment using regional cerebral blood flow SPECT. *NeuroImage* 2005; 28: 1014-1021.
6. Friston KJ, Ashburner J, Frith CD et al. Spatial registration and normalization of images. *Human Brain Mapping* 1995; 2: 165-189.
7. Friston KJ, Holmes AP, Worsley KJ et al. Statistical parametric maps in functional imaging: A general linear approach. *Human Brain Mapping* 1995; 2: 189-210.
8. Poline JB, Worsley KJ, Himes AP et al. Estimating smoothness in statistical parametric maps: Variability of p values. *J Comput Assist Tomogr* 1995; 19: 788-796.
9. Ashburner J, Friston KJ. Nonlinear spatial normalization using basis functions. *Human Brain Mapping* 1999; 7: 254-266.
10. Minoshima S, Koeppe RA, Frey KA, Kuhl DE. Anatomic standardization: Linear scaling and nonlinear warping of function brain images. *J Nucl Med* 1994; 35: 1528-1537.
11. Minoshima S, Frey KA, Koeppe RA et al. A diagnostic approach in Alzheimer's disease using three-dimensional stereotactic surface projections of fluorine-18-FDG PET. *J Nucl Med* 1995; 36: 1238-1248.
12. Matsuda H, Mizumura S, Soma T, Takemura N. Conversion of brain SPECT images between different collimator and reconstruction processes for analysis using statistical parametric mapping. *Nucl Med Commun* 2004; 25: 67-74.
13. Kanetaka H, Matsuda H, Asada T et al. Effects of partial volume correction on discrimination between very early Alzheimer's dementia and controls using brain perfusion SPECT. *Eur J Nucl Med Mol Imaging* 2004; 31: 975-980.
14. Mase S, Takeda J. Spatial data modeling: Data science series 7. *Kyoritsu Publishing* 2002; Tokyo, Ritei Shibata, 59-117. (in Japanese)
15. Besag J. Spatial interaction and the statistical analysis of lattice systems. *J R Statist Soc. B* 1974; 36: 192-236.
16. Geman S, Geman D. Stochastic relaxation, Gibbs distributions, and the Bayesian restoration of images. *IEEE Transact on Pattern Anal and Machine Intellig* 1984; 6: 721-741.
17. Smith AFM, Roberts GO. Bayesian computation via the Gibbs sampler and related Markov chain Mote Carlo methods. *J R Statist Soc B* 1993; 55: 3-23.
18. Tierney L. Markov chains for exploring posterior distribution. *Ann Statistics* 1994; 22: 1701-1762.
19. Cowels MK, Carlin BP. Markov chain Monte Carlo convergence diagnostics: A comparative review. *J Amer Statist Assoc* 1996; 91: 883-904.
20. Cowels MK, Roberts GO, Rosenthal JS. Possible biases induced by MCMC convergence diagnostics. *J Statist Comput Siml* 1999; 64: 87-104.
21. Jones GL, Hobert JP. Sufficient burn-in for Gibbs samplers for a hierarchical random effects model. *Ann Statistics* 2004; 32: 784-817.
22. Duchon J. Spline minimizing rotation invariant seminorms in sobolev spaces. *Constructive theory of functions of several variables* 1976; 1: 85-100.
23. Zheng X, Basher R. Thin-plate smoothing spline modeling oh spatial climate data and its application to mapping South Pacific rainfalls. *Amer Meteorol Science* 1995; 123: 3086-3102.
24. Baseg J, Green P, Higdon D, Mengersen K. Bayesian computation and stochastic systems. *Statistical Science* 1995; 10: 3-66.